THE JOURNAL OF BIOLOGICAL CHEMISTRY VOL. 286, NO. 12, pp. 10856–10863, March 25, 2011

Destruction of Amyloid Fibrils of Keratoepithelin Peptides by Laser Irradiation Coupled with Amyloid-specific Thioflavin T*[S]

Received for publication, January 18, 2011, and in revised form, January 18, 2011 Published, JBC Papers in Press, February 7, 2011, DOI 10.1074/jbc.M111.222901

Daisaku Ozawa[‡1], Yuichi Kaji[§1], Hisashi Yagi[‡], Kazumasa Sakurai[‡], Toru Kawakami[‡], Hironobu Naiki[¶], and Yuji Goto[‡2]

From the [‡]Institute for Protein Research, Osaka University, Yamadaoka 3-2, Suita, Osaka 565-0871, Japan, the [§]Department of Ophthalmology, Institute of Clinical Medicine, University of Tsukuba, Ibaraki 305-8575, Japan, and the [¶]Department of Pathological Sciences, Faculty of Medical Sciences, University of Fukui, Matsuoka, Fukui 910-1193, Japan

Mutations in keratoepithelin are associated with blinding ocular diseases, including lattice corneal dystrophy type 1 and granular corneal dystrophy type 2. These diseases are characterized by deposits of amyloid fibrils and/or granular non-amyloid aggregates in the cornea. Removing the deposits in the cornea is important for treatment. Previously, we reported the destruction of amyloid fibrils of β_2-microglobulin K3 fragments and amyloid β by laser irradiation coupled with the binding of an amyloid-specific thioflavin T. Here, we studied the effects of this combination on the amyloid fibrils of two 22-residue fragments of keratoepithelin. The direct observation of individual amyloid fibrils was performed in real time using total internal reflection fluorescence microscopy. Both types of amyloid fibrils were broken up by the laser irradiation, dependent on the laser power. The results suggest the laser-induced destruction of amyloid fibrils to be a useful strategy for the treatment of these corneal dystrophies.

A number of proteins and peptides have been found to aggregate into insoluble amyloid fibrils that are involved in various diseases, including Alzheimer's disease, Parkinson's disease, and dialysis-related amyloidosis (1–5). Keratoepithelin is one of the amyloidogenic proteins responsible for blinding corneal dystrophies (6–9). Although precursor proteins range from native globular proteins to unstructured peptides, the resultant amyloid fibrils have many characteristics in common (1–4). Amyloid fibrils are typically long, unbranched, and often twisted, consisting of several protofilaments. X-ray fiber diffraction experiments have shown that they are commonly constructed from ordered β-strands. The basic structure has been considered a cross-β structure in which the β-strands are located perpendicular to the fibril axis. In addition, amyloid fibrils exhibit specific optical behavior such as green birefringence when bound to the dye Congo red. They also bind to the fluorescence dye thioflavin T (ThT)[3], resulting in a characteristic fluorescence emission at 482–490 nm with an excitation maximum at 446–455 nm (10, 11).

Hereditary corneal dystrophies are characterized by the abnormal deposition of amyloid fibrils and/or granular aggregation in the cornea (6–9). Mutations of keratoepithelin, an extracellular matrix protein composed of 683 amino acids, also known as transforming growth factor β-induced (TGFβI), are responsible for the dystrophies. Population analyses have revealed two hot spots of mutation, Arg-124 and Arg-555, associated with corneal dystrophies (7, 12). Regarding Arg-124, four different mutations are associated with four different phenotypes. The R124C mutation has been linked with lattice corneal dystrophy type 1, R124H with granular corneal dystrophy type 2, R124L with granular corneal dystrophy type 3, and R124S with a variant of granular corneal dystrophy type 1. Despite numerous studies, an effective therapeutic approach for these corneal dystrophies has yet to be established (9).

Recently, several groups have studied ways to treat amyloidosis. Various inhibitors acting in the initial stages of amyloid β (Aβ) fibril formation have been reported (13–15). Drugs that increase the stability of the native state and/or kinetic barrier to amyloid fibrils have been developed for transthyretin amyloidoses (16, 17). However, the development of a novel strategy for destroying preformed amyloid fibrils is also desired.

To study amyloid fibrils, we developed a unique technique for their direct observation, which combines total internal reflection fluorescence microscopy (TIRFM) with an amyloid-specific ThT (18–22). The approach can provide important information about the morphology, growth rate, and direction of extension of individual fibrils in real time. Using this method, we previously observed the laser irradiation-dependent inhibition of β_2-microglobulin fibril growth and the destruction of preformed fibrils of K3, a 22-residue peptide of β_2-microglobulin (23). More recently, we examined the effects of laser irradiation on the formation of Aβ(1–40) fibrils (24). As was the case for K3 fibrils, extensive irradiation destroyed the preformed Aβ fibrils. However, irradiation during the formation of fibrils resulted in only the partial destruction of growing fibrils and a subsequent explosive propagation of fibrils, leading to a bell-

* This work was supported by Grants-in-aid from the Japanese Ministry of Education, Culture, Sports, and Science and Technology and by a Research Fellowship for Young Scientists from the Japan Society for the Promotion of Science (to H. Y.).

[S] The on-line version of this article (available at http://www.jbc.org) contains a supplemental movie.

[1] Both authors contributed equally to this work.

[2] To whom correspondence should be addressed: Yamadaoka 3-2, Suita, Osaka 565-0871, Japan. Tel.: 81-6-6879-8614; Fax: 81-6-6879-8616; E-mail: ygoto@protein.osaka-u.ac.jp.

[3] The abbreviations used are: ThT, thioflavin T; Aβ, amyloid β; C110–131 and H110–131, synthetic 22-residue peptides covering Leu110-Glu131 of keratoepithelin sequence with R124C and R124H mutations, respectively; TIRFM, total internal reflection fluorescence microscopy; mW, milliwatt.

shaped profile of propagation against the laser energy. The explosive propagation was caused by an increase in the number of active ends because of breakage. We propose that the effects of the irradiation are determined by a balance between the laser-induced acceleration of propagation and the destruction.

The results suggest, keeping the bell-shaped profile in mind, that the laser-induced destruction of amyloid fibrils coupled with an amyloid-specific dye is useful in the treatment or prevention of amyloid-related diseases, for which no effective method has yet been established. However, it is still unclear whether amyloid fibrils other than K3 and Aβ(1–40) fibrils are destroyed by laser irradiation.

Previously, using a synthetic 22-residue peptide covering Leu-110-Glu-131 of the keratoepithelin sequence and mutant versions with R124C and R124H mutations, called C110–131 and H110–131 peptides, respectively (Fig. 1*A*), Schmitt-Bernard *et al.* (8) showed that these mutations increase the amyloidgenicity of the wild-type peptide, suggesting an underlying mechanism of the Arg-124 mutation-linked corneal dystrophies. In this paper, we examine the effects of laser irradiation on the amyloid fibrils of these mutant peptides. The results show that, similar to K3 and Aβ(1–40) fibrils, both C110–131 and H110–131 fibrils were broken up by the laser irradiation. This approach may become a new therapeutic strategy for destroying amyloid fibrils in corneal dystrophies as well as other amyloid-related diseases.

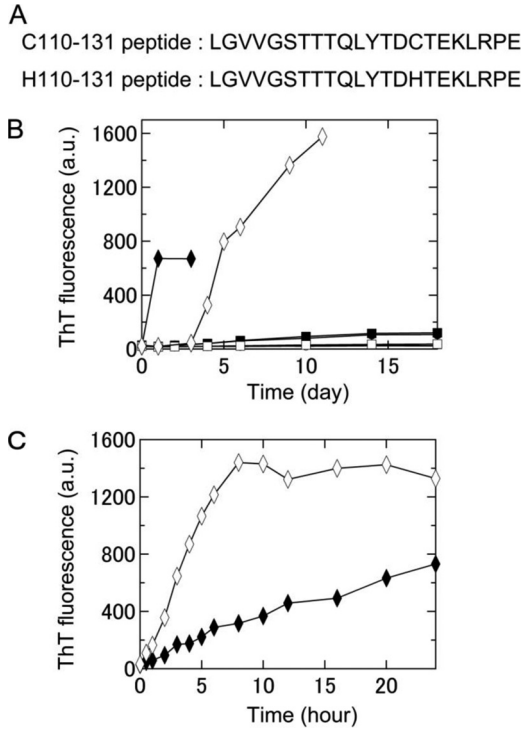

FIGURE 1. **Formation of amyloid fibrils of two keratoepithelin peptide fragments, C110–131 and H110–131, under various conditions at neutral pH monitored using ThT fluorescence.** *A*, amino acid sequences of the C110–131 and H110–131 peptides. *B*, time course of the spontaneous formation of C110–131 (▲, ●, ■, ♦) and H110–131 (△, ○, □, ◇) fibrils in 67 mM sodium phosphate buffer (pH 7.4) at 4 °C (▲, △), 67 mM sodium phosphate buffer (pH 7.4) at 37 °C (●, ○), 50 mM sodium phosphate buffer (pH 7.0) containing 100 mM NaCl at 37 °C (■, □), or 50 mM sodium phosphate buffer (pH 7.0) containing 100 mM NaCl and 0.5 mM SDS at 37 °C (♦, ◇). *C*, time course of seed-dependent growth of C110–131 (♦) and H110–131 (◇) peptides in 50 mM sodium phosphate buffer (pH 7.0) containing 100 mM NaCl and 0.5 mM SDS at 37 °C. Concentration of seeds was 5 μg/ml.

EXPERIMENTAL PROCEDURES

Formation of Amyloid Fibrils—Chemically synthesized C110–131 and H110–131 peptides were purchased from the Peptide Institute, Inc. (Osaka, Japan). The peptides were dissolved in 100% dimethyl sulfoxide and then diluted into the buffer solutions. The final concentration of dimethyl sulfoxide was less than 1% (v/v). For the spontaneous formation of fibrils, the peptides at 400 μM were incubated in 67 mM sodium phosphate (pH 7.4) at 4 °C, 67 mM sodium phosphate (pH 7.4) at 37 °C, 50 mM sodium phosphate (pH 7.0) containing 100 mM NaCl at 37 °C, or 50 mM sodium phosphate (pH 7.0) containing 100 mM NaCl and 0.5 mM SDS at 37 °C. In the case of seed-dependent growth, each seed was prepared by the fragmentation of preformed amyloid fibrils with a TAITEC VP-30S sonicator (Saitama, Japan) equipped with a microtip. The seeds were added at a final concentration of 5 μg/ml to 400 μM peptides in 50 mM sodium phosphate (pH 7.0) containing 100 mM NaCl and 0.5 mM SDS at 37 °C.

ThT Fluorescence Assay—The formation of amyloid fibrils was monitored fluorometrically with ThT at 25 °C. The excitation and emission wavelengths were 445 and 485 nm, respectively. From each reaction tube, 5 μl was taken and mixed with 1 ml of 5 μM ThT in 50 mM glycine-NaOH buffer (pH 8.5), and the fluorescence of ThT was measured using a Hitachi F-7000 spectrofluorometer (Tokyo, Japan).

Direct Observation of Amyloid Fibrils—The TIRFM system used to observe individual amyloid fibrils was developed based on an inverted microscope (IX70, Olympus, Tokyo, Japan) as described (18–22). The ThT molecule was excited at 442 nm by a helium-cadmium laser (IK5552R-F, Kimmon, Tokyo, Japan). The laser power was 80 mW, and the observation period was 2 s. The fluorescence image was filtered with a bandpass filter (D490/30, Omega Optical, Bratteboro, VT) and visualized using a digital steel camera (DP70, Olympus).

Each peptide (400 μM) was incubated in 50 mM sodium phosphate (pH 7.0) containing 100 mM NaCl and 0.5 mM SDS. The ThT solution was then added at a final concentration of 10 μM. An aliquot (14 μl) of each sample was immediately deposited on a microscopic quartz slide, tightly sealed with a coverslip, and incubated at 37 °C, and an image of the fibrils was obtained with TIRFM.

Effects of the Laser Beam on Preformed Fibrils—To examine the effect of laser treatment, intermittent irradiation of C110–131 and H110–131 fibrils was performed. The fibrils formed on the quartz surface were irradiated by a helium-cadmium laser. The irradiation time was 2 s every 15 or 30 min, and the laser power was 80 mW. It should be noted that the laser irradiation points were also the observation points.

The fluorescence images of amyloid fibrils visualized with TIRFM were quantified to obtain the time course of their destruction. TIRFM images are made up of pixels with respective fluorescence intensities. For each image, a histogram of the fluorescence intensity was fitted using the multi-Gaussian method. Then, from the Gaussian peak with the lowest peak intensity, the average signal intensity of the background ($\langle I_{bkg} \rangle$)

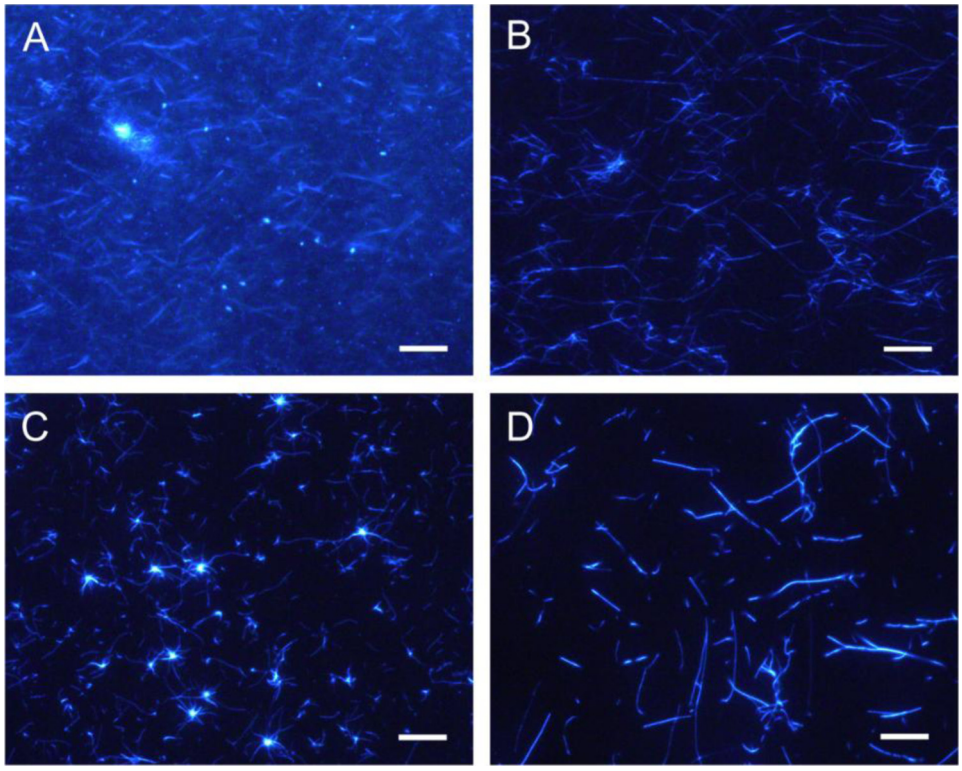

FIGURE 2. **Images of amyloid fibrils of two keratoepithelin peptide fragments observed by TIRFM.** TIRFM images of C110–131 (*A* and *C*) and H110–131 (*B* and *D*) fibrils in the presence of 100 mM NaCl and 0.5 mM SDS. C110–131 (*A*) and H110–131 (*B*) fibrils that extended spontaneously in test tubes were observed after incubation for 3 days and 11 days, respectively. C110–131 (*C*) and H110–131 (*D*) fibrils that extended seed-dependently on quartz slides were observed after incubation for 6 h. *Scale bars* = 10 μm.

and its standard deviation (σ_{bkg}) were obtained. The number of pixels whose intensity was greater than the threshold value of $<I_{bkg}> + 5\sigma_{bkg}$ was counted as the quantity of fibrils formed. The values obtained were normalized with respect to the highest value within each observation period.

Laser Irradiation to Preformed Fibrils in a Glass Cell—The C110–131 and H110–131 fibrils prepared by seed-dependent growth reactions were diluted 40-fold with 50 mM sodium phosphate (pH 7.0) containing 100 mM NaCl and 0.5 mM SDS. ThT was added at a final concentration of 10 μM. The samples were introduced into a glass cell with a 10-mm light path and then irradiated with a helium-cadmium laser continuously at 37 °C under agitation. The laser power was 60–80 mW. The irradiated fibrils were examined by monitoring ThT fluorescence (excitation 445 nm, emission 485 nm) and light scattering (both set at 350 nm) intensities. These measurements were made with a Hitachi F-4500 spectrofluorometer at 37 °C.

Transmission Electron Microscopy—The sample was spread on carbon-coated grids, negatively stained with 1% phosphotungstic acid (pH 7.0), and examined under a Hitachi H-7650 electron microscope with an acceleration voltage of 80 kV.

High-pressure Liquid Chromatography and Mass Analysis—The laser-irradiated fibrils were lyophilized and then dissolved in dimethyl sulfoxide. The sample was subjected to reverse-phased HPLC performed on a liquid chromatographer (Gilson, Inc., Middleton, WI) equipped with $5C_4$-AR-300 (4.6 mm × 150 mm; Nacalai Tesque, Inc., Kyoto, Japan). The sample was eluted with a gradient beginning with solvent A (0.05% trifluoroacetic acid) and an increasing percentage of solvent B (0.05% trifluoroacetic acid/acetonitrile) at a flow rate of 0.5 ml/min. All peaks were collected and lyophilized. Samples dissolved in water/acetonitrile (2:1) containing 0.1% trifluoroacetic acid were mixed with a matrix (α-cyano-4-hydroxy acid in water/acetonitrile (2:1) containing 0.1% trifluoroacetic acid at a ratio of 1:1, and then 2 μl was deposited onto a target plate. Matrix-assisted laser desorption ionization-time of flight mass spectrometry (Bruker Daltonics) was used for identification.

Amino Acid Analysis—Amino acid analysis was performed on a Hitachi L-2000 amino acid analyzer after hydrolysis with constant boiling point HCl at 110 °C for 24 h in an evacuated sealed tube. HPLC was carried out on a cation ion exchange column. The amino acids were detected by the reaction with ninhydrin.

RESULTS

Direct Observation of Amyloid Fibrils of Keratoepithelin Peptide Fragments—Previously, Schmitt-Bernard *et al.* (8) showed the spontaneous fibril formation of the synthetic peptides C110–131 and H110–131 using an *in vitro* dialysis-based approach. To observe individual amyloid fibrils with TIRFM, we searched for the best conditions for the spontaneous formation of fibrils of C110–131 and H110–131 peptides. The fibrils were generated at a neutral pH, based on buffer conditions established previously (8), and the process was monitored with a ThT-binding assay. At 4 °C, the intensity of ThT fluorescence did not increase for either peptide (Fig. 1*B*). At 37 °C, the fluorescence increased gradually for the C110–131 peptide but not at all for the H110–131 peptide. We then added NaCl and SDS,

which are known to enhance fibril growth (22, 24). The intensity of ThT fluorescence of both these peptides increased markedly in the presence of 100 mM NaCl and 0.5 mM SDS (Fig. 1*B*). Fibrils of the H110–131 peptide formed slower than those of the C110–131 peptide. TIRFM images revealed a large number of C110–131 and H110–131 fibrils (Fig. 2, *A* and *B*). Therefore, in subsequent experiments, we included 100 mM NaCl and 0.5 mM SDS for fibril growth. It is likely that a low concentration of SDS mimics the membrane environment *in vivo*.

A long incubation period (> 3 days) on glass slides tended to dry the samples out, making TIRFM experiments difficult. Because the spontaneous formation of H110–131 fibrils required more than 3 days (Fig. 1*B*), we examined the seed-dependent growth of C110–131 and H110–131 fibrils. The seeds were prepared by fragmenting preformed fibrils with a sonicator (see "Experimental Procedures"). In the presence of seeds, the fibril growth of both C110–131 and H110–131 peptides occurred without a lag phase (Fig. 1*C*). Moreover, the seed-dependent fibril growth of these peptides occurred on quartz slides as revealed by TIRFM (Fig. 2, *C* and *D*). Radial growth patterns of the C110–131 fibrils were seen on the quartz slides after incubation for 12 h. In the case of H110–131, the fibrils tended to be longer than those of C110–131, suggesting that the mutations affect the supramolecular morphology of amyloid fibrils.

Destruction of Keratoepithelin Peptide Fibrils by Laser Irradiation—Using TIRFM, the destruction of C110–131 and H110–131 fibrils by laser irradiation was verified. The fibrils were preformed with seeds on quartz slides and then observed every 15 min (Fig. 3). For the observation, the fibrils were irradiated intermittently with a laser beam at a power of 80 mW and for a duration of 2 s. It should be noted that the irradiation points were also the observation points. At time zero, the preformed C110–131 fibrils were detected (Fig. 3*A*). With intermittent irradiation, the fibrils gradually decomposed and disappeared with time. Finally, only short fibrils remained. As was the case for K3 and Aβ fibrils, these results indicate that C110–131 fibrils were destroyed by the irradiation coupled with the excitation of ThT.

Next, the same experiment was carried out with fibrils of the H110–131 peptide (Fig. 3*B* and supplemental movie). Although H110–131 tended to form longer fibrils with clustered cores, the results were basically similar to those for C110–131 fibrils. As the irradiation proceeded, H110–131 fibrils were destroyed simultaneously at various sites in the view. However, the core regions of clustered fibrils resisted degradation.

To examine the dependence of the destruction of amyloid fibrils on the interval between bouts of irradiation (*i.e.* total laser beam dosage), H110–131 fibrils were irradiated for 2 s every 30 min instead of every 15 min (Fig. 3*C*). The fibrils were broken up more slowly when the irradiation was delivered every 30 min rather than every 15 min (Fig. 3*B*).

To see the dependence of the destruction on the dosage of irradiation, we quantified the fluorescence images of amyloid fibrils visualized with TIRFM (Fig. 3*D*, see also "Experimental Procedures"). It should be noted that the data points show all of the irradiation points. The fluorescence intensity of C110–131 and H110–131 fibrils obtained by TIRFM decreased with the

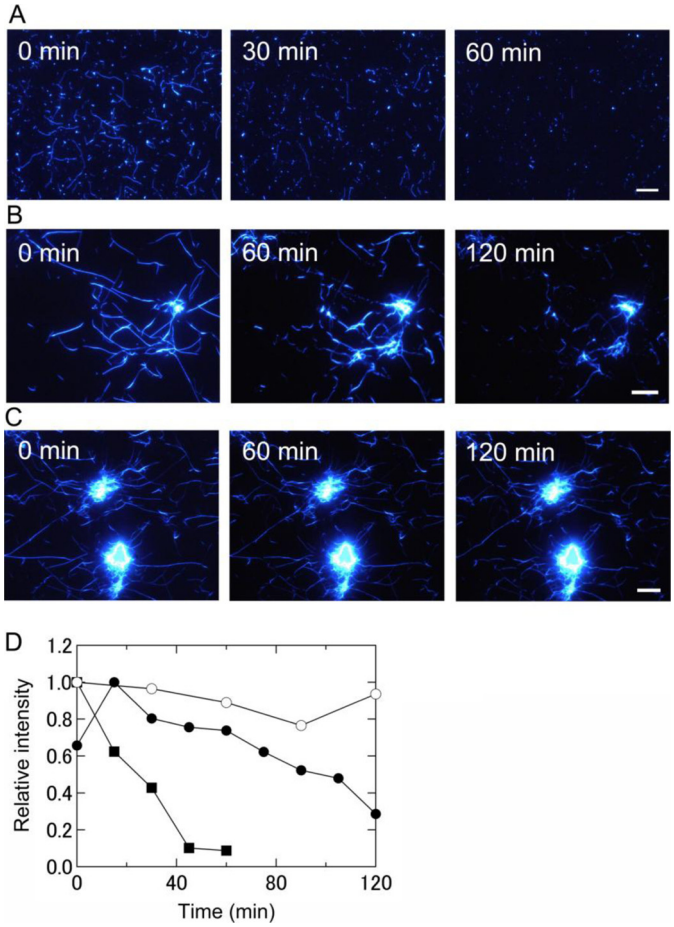

FIGURE 3. **Real-time observation by TIRFM of the destruction of keratoepithelin peptide fibrils by laser irradiation at pH 7. 0 and 37 °C.** *A*, C110–131 fibrils with 2 s of irradiation every 15 min. *B*, H110–131 fibrils with 2 s of irradiation every 15 min. *C*, H110–131 fibrils with 2 s of irradiation every 30 min. Fibrils were prepared on quartz slides in the absence of irradiation. *Scale bars* = 10 μm. *D*, the time courses of the destruction of these fibrils were obtained by quantifying TIRFM images (see "Experimental Procedures" for details). Shown are C110–131 fibrils with irradiation every 15 min ■, H110–131 fibrils with irradiation every 15 min (●), and H110–131 fibrils with irradiation every 30 min (○). The data points show all of the irradiation applied. The laser power was 80 mW.

number of times irradiation was applied (Fig. 3*D*). However, the decrease was faster for C110–131 fibrils, indicating that the clustered cores of H110–131 fibrils resisted degradation. Although the intensity of H110–131 fibrils irradiated every 15 min increased temporarily at 15 min, this is likely attributable to temporary fibril growth. However, the intensity was ultimately about half that at time zero. On the other hand, the decrease of intensity with irradiation every 30 min was slight. These results indicate that the destruction of fibrils depends on the dosage of irradiation.

Effects of Laser Irradiation on Keratoepithelin Peptide Fibrils in Bulk Solution—To further investigate the effects of laser irradiation on keratoepithelin peptide fibrils, we performed experiments in a bulk solution (Figs. 4-6). We first prepared C110–131 and H110–131 fibrils in a test tube. The fibrils were introduced into a glass cell with a 10-mm light path and then irradiated with a laser beam at 442 nm by a helium-cadmium laser at a power of 60–80 mW continuously under agitation with a stirrer tip.

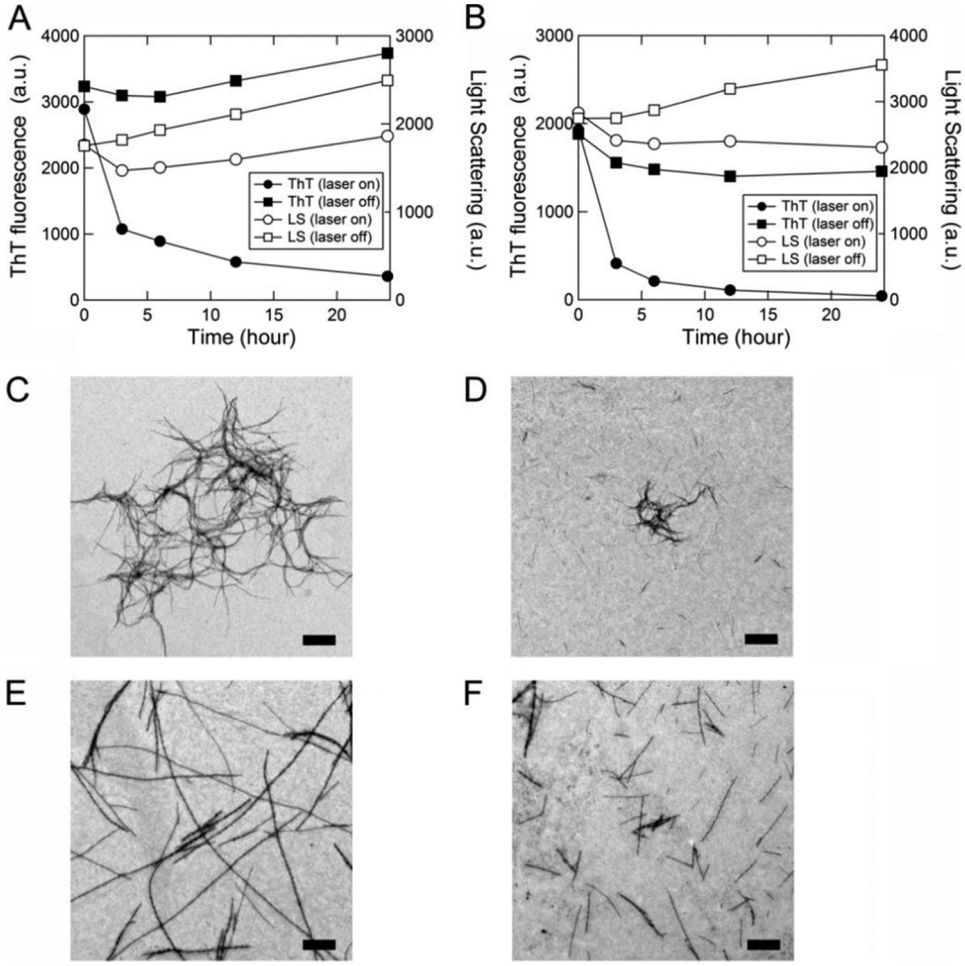

FIGURE 4. **Effects of laser-irradiation on keratoepithelin peptide fibrils in a glass cell monitored by ThT fluorescence, light scattering, and transmission electron microscopy.** *A* and *B*, kinetics of the decomposition of C110–131 (*A*) and H110–131 (*B*) fibrils were monitored using ThT fluorescence (●, ■) and light scattering (○, □) with (●, ○) or without (■, □) laser irradiation. *C–F*, electron microscopy images of C110–131 (*C* and *D*) and H110–131 (*E* and *F*) fibrils without laser irradiation (*C* and *E*) or after laser irradiation (*D* and *F*). *Scale bars* = 1 μm.

As the irradiation proceeded, the intensities of ThT fluorescence decreased (Fig. 4, *A* and *B*). The light scattering intensity of C110–131 fibrils decreased at 3 h and then gradually increased at 6 to 24 h (Fig. 4*A*). On the other hand, the light scattering intensity of H110–131 fibrils decreased at 3 to 24 h (Fig. 4*B*). In contrast, without irradiation, the light scattering intensities of both C110–131 and H110–131 fibrils did not decrease and rather increased at 3 to 24 h (Fig. 4, *A* and *B*). These results suggest that the destruction of keratoepithelin peptide fibrils was induced by laser irradiation in a bulk solution. The morphologies of keratoepithelin peptide fibrils with and without laser irradiation were monitored by transmission electron microscopy (Fig. 4, *C–F*). As shown by TIRFM (Fig. 2, *C* and *D*), the morphologies of C110–131 and H110–131 fibrils without laser irradiation were flexible and long straight structures, respectively (Fig. 4, *C* and *E*). However, after laser irradiation for 24 h, both C110–131 and H110–131 fibrils were broken down or decomposed into shorter fibrils (Fig. 4, *D* and *F*).

Analyses of the Laser-irradiated Keratoepithelin Peptide Fibrils—We then analyzed the chemical modifications of the laser-irradiated keratoepithelin peptide fibrils using reversed-phase HPLC (Fig. 5, *A* and *B*) and mass spectroscopy (Fig. 5, *C–F*). The irradiated keratoepithelin peptide fibrils were dissolved in dimethyl sulfoxide. The HPLC analyses of non-irradiated C110–131 and H110–131 fibrils revealed the peaks with retention times of 22 min and 21 min, corresponding to C110–131 and H110–131 monomers, respectively (Fig. 5, *A* and *B*). In contrast, the monomeric peak of irradiated C110–131 fibrils disappeared and that of irradiated H110–131 fibrils was significantly decreased in intensity. In the mass analysis, compared with the sample of C110–131 and H110–131 fibrils without irradiation (*m*/*z*, 2411 and 2446, respectively) (Fig. 5, *C* and *E*), the sample of irradiated C110–131 and H110–131 fibrils showed the peaks with a smaller molecular weight than the monomer (*m*/*z*, 872 and 629, respectively) (Fig. 5, *D* and *F*). These results indicated that the laser irradiation underwent the cleavage of peptide bonds and, moreover, various chemical modifications.

To examine the chemical modifications further, we performed amino acid analysis (Fig. 6, *A* and *B*). Our previous studies have shown that the His residue was modified by laser-induced active oxygen (23, 24). Cys, Met, Tyr, His, and Trp are susceptible to oxidation. The C110–131 peptide contains one Tyr and one Cys residue, and the H110–131 peptide contains one Tyr and one His residue (Fig. 1*A*). The content of His residue in the irradiated H110–131 fibrils decreased to about

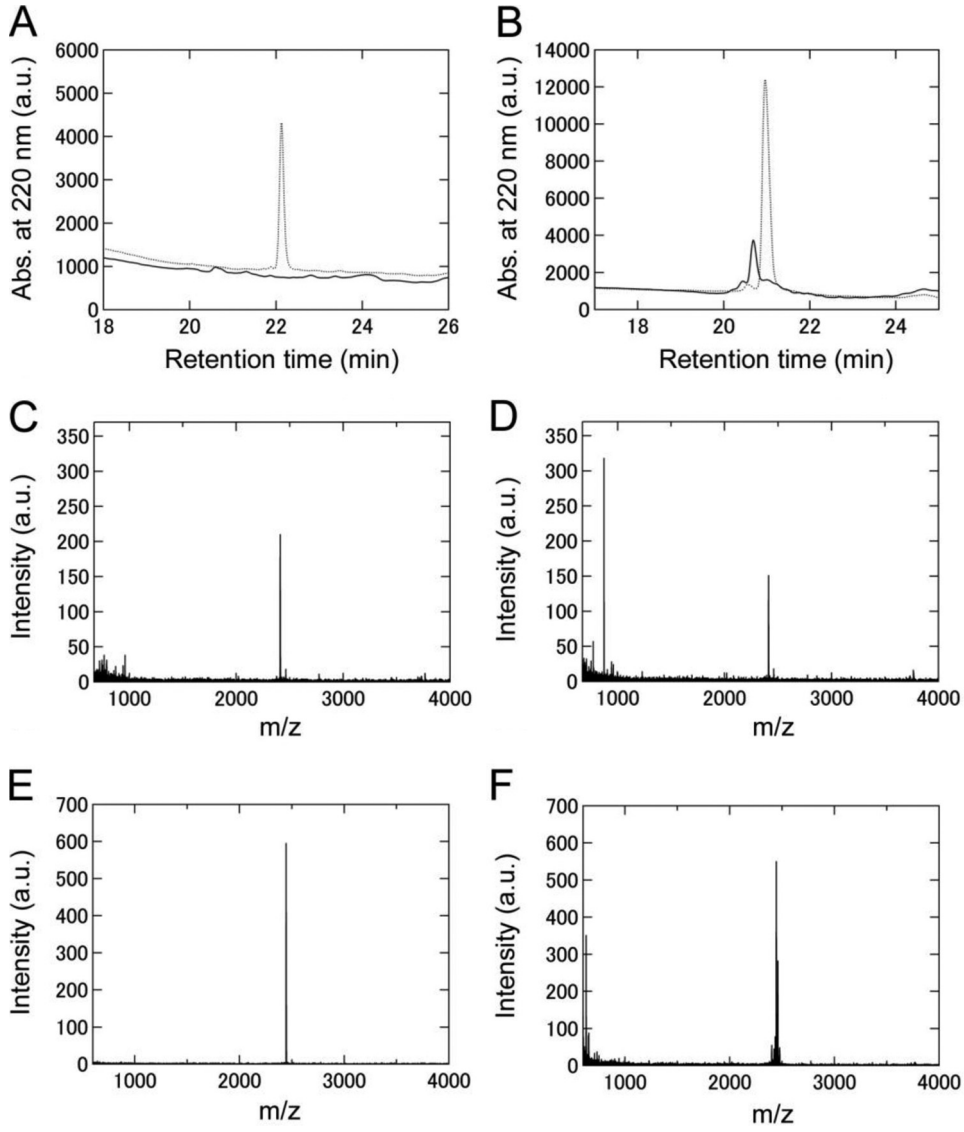

FIGURE 5. **Analyses of the laser-irradiated keratoepithelin peptide fibrils by reversed-phase HPLC and mass spectrometry.** *A* and *B*, elution profiles of C110–131 (*A*) and H110–131 (*B*) fibrils without laser irradiation (*dotted line*) or after laser irradiation (*solid line*) monitored by reversed-phase HPLC. Keratoepithelin peptide fibrils dissolved in dimethyl sulfoxide were injected. *C–F*, mass spectra of C110–131 (*C* and *D*) and H110–131 (*E* and *F*) fibrils without laser irradiation (*C* and *E*) or after laser irradiation (*D* and *F*). For all of *A–G*, the irradiation period was 24 h.

50–60% of the reference sample without irradiation after the irradiation for 3 and 6 h (Fig. 6*B*). Although the contents of Tyr and Cys residue in the irradiated C110–131 and H110–131 fibrils were not quantitatively determined, the contents of other residues remained almost unchanged after laser irradiation (Fig. 6, *A* and *B*). Thus, these results suggest that the Cys, Tyr, and His residues were modified by active oxygen.

DISCUSSION

Amyloid Fibrils of Keratoepithelin Peptides—To observe individual amyloid fibrils with TIRFM, we first examined the spontaneous formation of C110–131 and H110–131 fibrils. Both the peptides formed amyloid fibrils spontaneously in the presence of 100 mM NaCl and 0.5 mM SDS (pH 7.4) (Fig. 1*B*). The lag phase for the H110–131 peptide was 3 days, whereas C110–131 formed amyloid fibrils after 1 day. Moreover, the seed-dependent growth of the C110–131 peptide was faster than that of the H110–131 peptide (Fig. 1*C*). For several amyloidogenic peptides and proteins, the formation of intermolecular disulfide bonds has been shown to accelerate the fibril formation (25). In fact, a previous study on the C110–131 peptide indicated that the disulfide bond has an important role in the formation of amyloid fibrils (8). Thus, these results suggest that the intermolecular disulfide bonds formed by Cys residues in C110–131 accelerated the development of fibrils.

TIRFM images of the seed-dependent growth on quartz slides indicated that H110–131 fibrils are longer and straighter than C110–131 fibrils (Fig. 2, *C* and *D*). Similar to the TIRFM observations, electron microscopy images also revealed that the morphologies of C110–131 and H110–131 fibrils were flexible and long straight structures, respectively (Fig. 4, *C* and *E*). The different mutations of Arg-124 in keratoepithelin are known to be linked to different phenotypes of corneal dystrophies (7, 8). The R124C mutation has been associated with lattice corneal

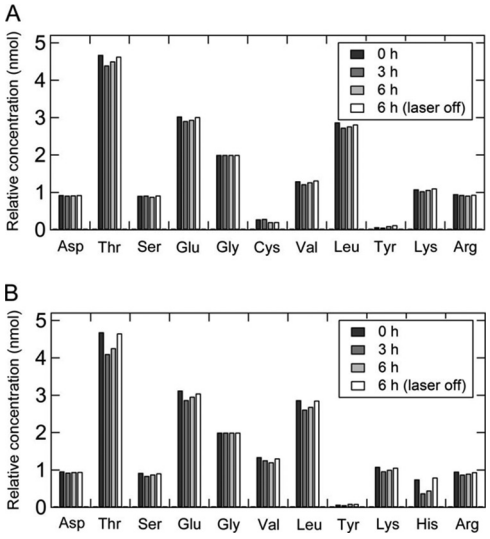

FIGURE 6. **Amino acid analysis of C110–131 (*A*) and H110–131 (*B*) fibrils before and after laser irradiation.**

dystrophy type 1 and R124H with granular corneal dystrophy type 2. Thus, the observed differences in the morphology of fibrils might reflect the characteristics of the various corneal dystrophies.

Laser-induced Destruction of Keratoepithelin Peptide Fibrils—We revealed that the amyloid fibrils of two keratoepithelin peptide fragments are decomposed by irradiation with a laser beam at 442 nm. The mechanism of destruction is thought to be similar to that for photodynamic therapy, a cancer treatment, which involves the use of photochemical reactions mediated through the interaction of light, photosensitizing agents, and molecular oxygen (26, 27). The reactions in the present study require ThT, indicating that laser-excited ThT plays an important role. Given previous results with the K3 peptide of β_2-microglobulin and Aβ(1–40) (23, 24), the laser-dependent destruction can be explained as follows.

The excited ThT transfers its energy to ground-state molecular oxygen, and singlet oxygen is produced. Labile singlet oxygen attacks directly the side chains of amino acid residues in amyloid fibrils. During the destruction of K3 and Aβ(1–40) fibrils, we reported that the His residues were damaged by laser irradiation (23, 24). In fact, after laser irradiation, the His content in the irradiated H110–131 fibrils clearly decreased (Fig. 6*B*). However, it has remained unclear whether other amino acid residues were also damaged. Cys, Met, Tyr, His, and Trp have been shown to be most vulnerable to modifications by photooxidation (28, 29). Among the keratoepithelin peptide fragments, C110–131 contains one Tyr and one Cys residue, and H110–131 contains one Tyr and one His residue. Although the C110–131 peptide has no His residues, the amyloid fibrils of C110–131 were effectively destroyed by the irradiation (Figs. 3 and 4). These results suggest that amino acid residues other than His (*i.e.* Cys, Met, Tyr, and Trp) are also broken up by the laser in the presence of amyloid-bound ThT, confirming the approach to be applicable to various types of amyloid fibrils with distinct sequences. Moreover, because the destruction of both C110–131 and H110–131 fibrils were induced by laser irradiation, the laser-induced destruction may be efficacious in the various morphologies of amyloid fibrils.

Possible Treatment of Corneal Dystrophies with Laser Irradiation—Our results suggest that the laser-induced destruction of amyloid fibrils coupled with an amyloid-specific dye is useful for the treatment or prevention of amyloid-related diseases (23). However, with Aβ(1–40), we also observed an accelerating effect of the laser on propagation after the apparent inhibition or destruction of growing fibrils (24). Although this was unexpected, the mechanism is straightforward: The breaking up of preformed fibrils increases the number of active ends, thus leading to an acceleration of fibril growth. Thus, the growth of fibrils under irradiation is a dynamic process determined by a balance between the destruction of preformed fibrils and a partial destruction-triggered acceleration of fibril growth. In other words, the formation or degradation of fibrils can be achieved by manipulating laser power and duration.

Laser treatment has been developed for several ocular diseases. For example, verteporfin, a photosensitizing agent excited at 689 nm, is used to treat age-related macular degeneration (30). The wavelength for excitation in photodynamic therapy is determined by the selection of photosensitizing agents. Furthermore, the depth for which the laser penetrates tissue depends on the wavelength of the light (26). For example, a long-wavelength light (from 600 to 700 nm) penetrates 50–200% further than a short-wavelength light (from 400 to 500 nm). However, it is generally difficult to deliver laser light to the tissues where amyloid fibrils deposit (*i.e.* brain, heart, kidneys, and joints). On the other hand, because the thickness of the cornea is about 0.5 mm in the center and about 0.7 mm at the periphery, laser light in the 400–500 nm regions can be delivered to amyloid fibrils in cases of corneal dystrophy. Thus, we expect, by finding or developing photosensitizing agents with similar characteristics to ThT, that the laser-induced destruction of amyloid fibrils will become a powerful therapeutic strategy for corneal dystrophies.

Moreover, photodynamic therapy has been considered to be a promising treatment for cancer, even though the cancer tissues are usually not directly accessible to the laser beams (26, 27). For the same reason, by pursuing the methodology of applying the laser beams to various types of amyloid deposits, the laser beam-dependent destruction can become a general therapeutic approach against amyloidoses.

CONCLUSION

In conclusion, we demonstrated that a laser destroyed amyloid fibrils of keratoepithelin peptide fragments in the presence of amyloid-specific ThT. This approach should apply to amyloid fibrils with His, Cys, Tyr, Met, and/or Trp residues, particularly with ocular diseases where amyloid-like deposits are accessible to irradiation. Moreover, the fine-tuning of laser treatment in terms of hardware and software has been achieved in the field of ocular research. Although further studies are necessary, we suggest, keeping the possible bell-shaped profile of the laser-energy-dependent propagation and destruction of amyloid fibrils in mind, that this approach will be a promising

therapeutic strategy for the treatment and prevention of corneal dystrophies.

Acknowledgments—We thank Drs. Tetsuichi Wazawa (Tohoku University) and Tadato Ban (Fukui University) for support with the TIRFM system.

REFERENCES

1. Dobson, C. M. (2003) *Nature.* **426,** 884–890
2. Cohen, F. E., and Kelly, J. W. (2003) *Nature.* **426,** 905–909
3. Uversky, V. N., and Fink, A. L. (2004) *Biochim. Biophys. Acta.* **1698,** 131–153
4. Chiti, F., and Dobson, C. M. (2006) *Annu. Rev. Biochem.* **75,** 333–366
5. Stoppini, M., Andreola, A., Foresti, G., and Bellotti, V. (2004) *Pharmacol. Res.* **50,** 419–431
6. Schmitt-Bernard, C. F., Chavanieu, A., Derancourt, J., Arnaud, B., Demaille, J. G., Calas, B., and Argiles, A. (2000) *Biochem. Biophys. Res. Commun.* **273,** 649–653
7. Korvatska, E., Henry, H., Mashima, Y., Yamada, M., Bachmann, C., Munier, F. L., and Schorderet, D. F. (2000) *J. Biol. Chem.* **275,** 11465–11469
8. Schmitt-Bernard, C. F., Chavanieu, A., Herrada, G., Subra, G., Arnaud, B., Demaille, J. G., Calas, B., and Argilés, A. (2002) *Eur. J. Biochem.* **269,** 5149–5156
9. Yuan, C., Berscheit, H. L., and Huang, A. J. (2007) *FEBS Lett.* **581,** 241–247
10. Naiki, H., Higuchi, K., Hosokawa, M., and Takeda, T. (1989) *Anal. Biochem.* **177,** 244–249
11. Biancalana, M., Makabe, K., Koide, A., and Koide, S. (2009) *J. Mol. Biol.* **385,** 1052–1063
12. Korvatska, E., Munier, F. L., Djemaï, A., Wang, M. X., Frueh, B., Chiou, A. G., Uffer, S., Ballestrazzi, E., Braunstein, R. E., Forster, R. K., Culbertson, W. W., Boman, H., Zografos, L., and Schorderet, D. F. (1998) *Am. J. Hum. Genet.* **62,** 320–324
13. Walsh, D. M., Townsend, M., Podlisny, M. B., Shankar, G. M., Fadeeva, J. V., El Agnaf, O., Hartley, D. M., and Selkoe, D. J. (2005) *J. Neurosci.* **25,** 2455–2462
14. LeVine, H., 3rd. (2007) *Amyloid.* **14,** 185–197
15. Esteras-Chopo, A., Morra, G., Moroni, E., Serrano, L., Lopez de la Paz, M., and Colombo, G. (2008) *J. Mol. Biol.* **383,** 266–280
16. Sekijima, Y., Kelly, J. W., and Ikeda, S. (2008) *Curr. Pharm. Des.* **14,** 3219–3230
17. Miller, S. R., Sekijima, Y., and Kelly, J. W. (2004) *Lab. Invest.* **84,** 545–552
18. Ban, T., Hamada, D., Hasegawa, K., Naiki, H., and Goto, Y. (2003) *J. Biol. Chem.* **278,** 16462–16465
19. Ban, T., Hoshino, M., Takahashi, S., Hamada, D., Hasegawa, K., Naiki, H., and Goto, Y. (2004) *J. Mol. Biol.* **344,** 757–767
20. Ban, T., Morigaki, K., Yagi, H., Kawasaki, T., Kobayashi, A., Yuba, S., Naiki, H., and Goto, Y. (2006) *J. Biol. Chem.* **281,** 33677–33683
21. Ban, T., Yamaguchi, K., and Goto, Y. (2006) *Acc. Chem. Res.* **39,** 663–670
22. Yagi, H., Ban, T., Morigaki, K., Naiki, H., and Goto, Y. (2007) *Biochemistry* **46,** 15009–15017
23. Ozawa, D., Yagi, H., Ban, T., Kameda, A., Kawakami, T., Naiki, H., and Goto, Y. (2009) *J. Biol. Chem.* **284,** 1009–1017
24. Yagi, H., Ozawa, D., Sakurai, K., Kawakami, T., Kuyama, H., Nishimura, O., Shimanouchi, T., Kuboi, R., Naiki, H., and Goto, Y. (2010) *J. Biol. Chem.* **285,** 19660–19667
25. Ohhashi, Y., Hasegawa, K., Naiki, H., and Goto, Y. (2004) *J. Biol. Chem.* **279,** 10814–10821
26. Giuliano, E. A., Ota, J., and Tucker, S. A. (2007) *Vet. Ophthalmol.* **10,** 337–343
27. Buytaert, E., Dewaele, M., and Agostinis, P. (2007) *Biochim. Biophys. Acta.* **1776,** 86–107
28. Agon, V. V., Bubb, W. A., Wright, A., Hawkins, C. L., and Davies, M. J. (2006) *Free Radic. Biol. Med.* **40,** 698–710
29. Davies, M. J. (2004) *Photochem. Photobiol. Sci.* **3,** 17–25
30. Augustin, A. J., and Schmidt-Erfurth, U. (2006) *Ophthalmology* **113,** 14–22